JACS
JOURNAL OF THE AMERICAN CHEMICAL SOCIETY

ARTICLE

pubs.acs.org/JACS

Anion Conductive Block Poly(arylene ether)s: Synthesis, Properties, and Application in Alkaline Fuel Cells

Manabu Tanaka,[†,∥] Keita Fukasawa,[‡] Eriko Nishino,[§] Susumu Yamaguchi,[§] Koji Yamada,[§] Hirohisa Tanaka,[§] Byungchan Bae,[†] Kenji Miyatake,[*,†,‡] and Masahiro Watanabe[*,†]

[†]Fuel Cell Nanomaterials Center and [‡]Clean Energy Research Center, University of Yamanashi, 4 Takeda, Kofu 400-8510, Japan

[§]Daihatsu Motor Co. Ltd., Frontier Technology R&D Division, 3000 Ryuo, Gamo, Shiga 520-2593, Japan

Supporting Information

ABSTRACT: Anion conductive aromatic multiblock copolymers, poly(arylene ether)s containing quaternized ammonio-substituted fluorene groups, were synthesized via block copolycondensation of fluorene-containing (later hydrophilic) oligomers and linear hydrophobic oligomers, chloromethylation, quaternization, and ion-exchange reactions. The ammonio groups were selectively introduced onto the fluorene-containing units. The quaternized multiblock copolymers (QPEs) produced ductile, transparent membranes. A well-controlled multiblock structure was responsible for the developed hydrophobic/hydrophilic phase separation and interconnected ion transporting pathway, as confirmed by scanning transmission electron microscopic (STEM) observation. The ionomer membranes showed considerably higher hydroxide ion conductivities, up to 144 mS/cm at 80 °C, than those of existing anion conductive ionomer membranes. The durabilities of the QPE membranes were evaluated under severe, accelerated-aging conditions, and minor degradation was recognized by ^{1}H NMR spectra. The QPE membrane retained high conductivity in hot water at 80 °C for 5000 h. A noble metal-free direct hydrazine fuel cell was operated with the QPE membrane at 80 °C. The maximum power density, 297 mW/cm^2, was achieved at a current density of 826 mA/cm^2.

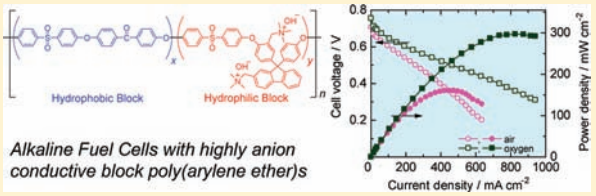

INTRODUCTION

For the past decade, there have been great demands for clean energy or renewable energy sources. Fuel cells are regarded as a promising candidate for stationary, automotive, and mobile applications because of their high energy density, high conversion efficiency, and low pollution levels.[1,2] Among the several kinds of fuel cells, most research efforts have been directed toward the development of polymer electrolyte fuel cells (PEFCs) using proton exchange membranes (PEMs) as the electrolyte.[3] Perfluorosulfonic acid polymers such as Nafion (DuPont) are state-of-the-art polymer electrolyte membranes for PEFCs. While the perfluorinated PEMs are highly proton conductive and are chemically, physically, and thermally stable, some significant drawbacks remain for widespread commercialization of PEFCs. These include environmental incompatibility and high production and processing costs of the perfluorinated materials. Besides, under strongly acidic conditions, precious metal-based electrocatalysts such as Pt are essential.

Recently, there has been a growing interest in alkaline fuel cells (AFCs) that utilize anion-exchange membranes (AEMs) as the electrolyte.[4−6] The advantages of AFCs over PEFCs include better kinetics of the oxygen reduction reaction and more options for cathode catalysts based on abundant transition metals such as nickel,[7,8] resulting in higher performance and lower cost fuel cells. Since the existing AEMs are not as ion conductive and stable as the PEMs, efforts have been devoted to developing better AEM materials. A variety of AEMs, whose main polymer chain structures range from poly(olefin)s,[9] poly(styrene)s,[10−12] poly(phenylene oxide)s,[13] poly(phenylene)s,[14] poly(ether imide)s,[15] poly(arylene ether)s,[16−21] to organic−inorganic hybrid composites,[22,23] have been investigated. Poly(arylene ether)s fall into a class of aromatic polymers that show good solubility in many organic solvents and distinguished membrane characteristics, and therefore have been widely used as the backbone of nonfluorinated PEMs. In the recent literature, poly(arylene ether)s were applied to AEMs by introducing quaternized ammonio,[16,17,19,21] guanidinio,[18] or phosphonio groups.[20] These AEMs are typically prepared by chloromethylation on aromatic rings or bromination on the methyl groups of the poly(arylene ether)s, followed by the Menshutkin reaction with tertiary amine, pentamethylguanidine, or tertiary phosphine to form benzylammonio, benzylguanidinio, or benzylphosphonio groups, respectively. We have synthesized poly(arylene ether)s containing ammonio group-substituted fluorene moieties (rQPE in Chart 1) and demonstrated their high anion conductivity and chemical and thermal stability.[24,25] The hydroxide ion conductivity reached 50 mS/cm at 30 °C and 78 mS/cm at 60 °C. The ionomer membranes owe such high ionic conductivity to the fluorene groups, which can carry up to four ionic groups per unit, to achieve high ion-exchange capacity (IEC).

Received: May 6, 2011
Published: June 09, 2011

Chart 1. Chemical Structure of Random Copoly(arylene ether)s Containing Ammonio Group-Substituted Fluorene Moieties (rQPE)

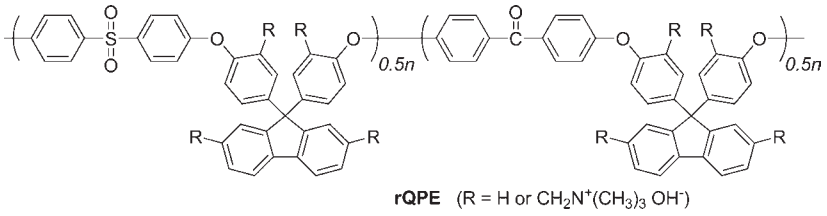

Scheme 1. Synthesis of Multiblock Copoly(arylene ether)s Containing Fluorene Groups (PEs)

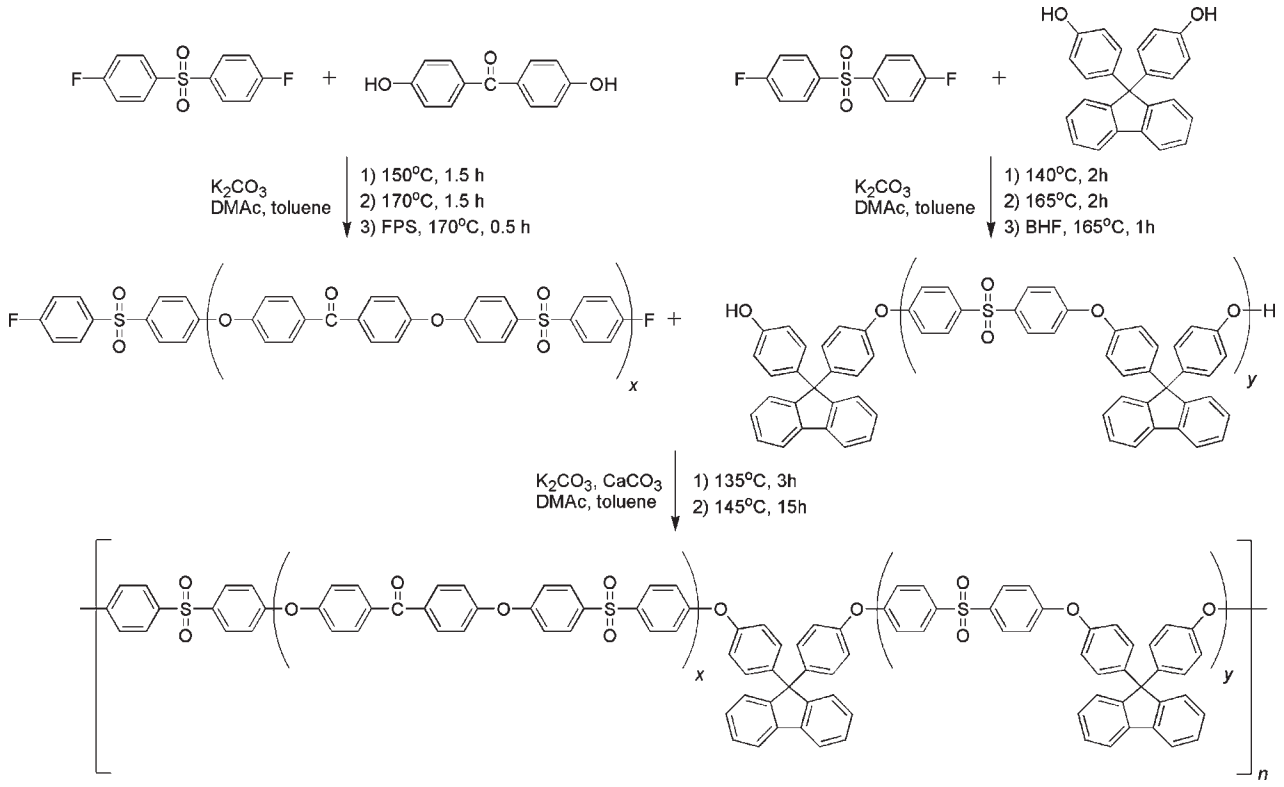

In the pursuit of alternative aromatic PEMs, we have proved that multiblock copolymers containing highly localized and dense sulfonic acid groups on fluorene groups in the hydrophilic blocks showed unique phase-separated morphology with well-interconnected proton transporting pathways. The sulfonated multiblock copolymer membranes were highly proton conductive at high temperature (110 °C) and showed fuel cell performance comparable to that of Nafion under severe conditions.[26−31] While there have been a few reports on AEMs based on block aromatic polymers,[21] the strategy of utilizing a sequential hydrophilic/hydrophobic structure with dense ionic groups in the hydrophilic blocks is also expected to be useful in AEMs. The objective of this research is to produce multiblock copoly(arylene ether)s containing quaternized ammonio groups and to evaluate their properties. For the synthesis, we have given careful consideration to the following points: to introduce ionic groups selectively at specific positions and to have as high an ionic density as possible in the hydrophilic segments. Both are crucial to make the most of multiblock architecture. By optimizing our previous results on the chloromethylation and quaternization reactions of poly(arylene ether) homopolymers and random copolymers,[24,25] the title multiblock copolymers, with well-controlled structure and composition, were successfully synthesized. Their water affinity, ion conductivity, mechanical properties, long-term durability, and alkaline fuel cell performance were investigated.

RESULTS AND DISCUSSION

Synthesis of Precursor Multiblock Copoly(arylene ether)s (PEs). A series of precursor multiblock copoly(arylene ether)s, PE-*X*8*Y*8, -*X*16*Y*11, -*X*22*Y*11, and -*X*22*Y*23 (numbers after *X* and *Y* represent the degrees of polymerization of the hydrophobic and fluorene-containing [later hydrophilic] blocks, respectively), were synthesized by nucleophilic substitution polycondensation of separately synthesized oligomers (Scheme 1). The hydrophobic oligomers, oligo(arylene ether sulfone ketone)s, were prepared by polycondensation of DHBP and FPS with a controlled feed monomer ratio (e.g., DHBP/FPS = 8/9 molar ratio

dx.doi.org/10.1021/ja204166e |*J. Am. Chem. Soc.* 2011, 133, 10646–10654

Table 1. Molecular weights of the multiblock PEs

	expected *X*/*Y* oligomer length	obtained *X*/*Y* oligomer length	M_n (kg/mol)	M_w (kg/mol)	M_w/M_n
PE-*X*8*Y*8	8/8	8/8	89	183	2.1
PE-*X*16*Y*11	16/16	16/11	54	93	1.7
PE-*X*22*Y*11	32/16	22/11	84	195	2.3
PE-*X*22*Y*23	32/32	22/23	90	159	1.8

for an $X = 8$ oligomer) in the presence of potassium carbonate in dry *N*,*N*-dimethylacetamide (DMAc) solution. In the last stage of the oligomerization reaction, a small amount of FPS was added to ensure the end-capping of the oligomers with F-terminal groups. The fluorene-containing oligomers with OH-terminal groups were prepared similarly from FPS and a controlled excess amount of BHF. The chemical structure and molecular weight of the hydrophobic and fluorene-containing oligomers were characterized by ^{1}H NMR spectra and GPC measurements (see Figure S1 and Table S1 in Supporting Information [SI]).

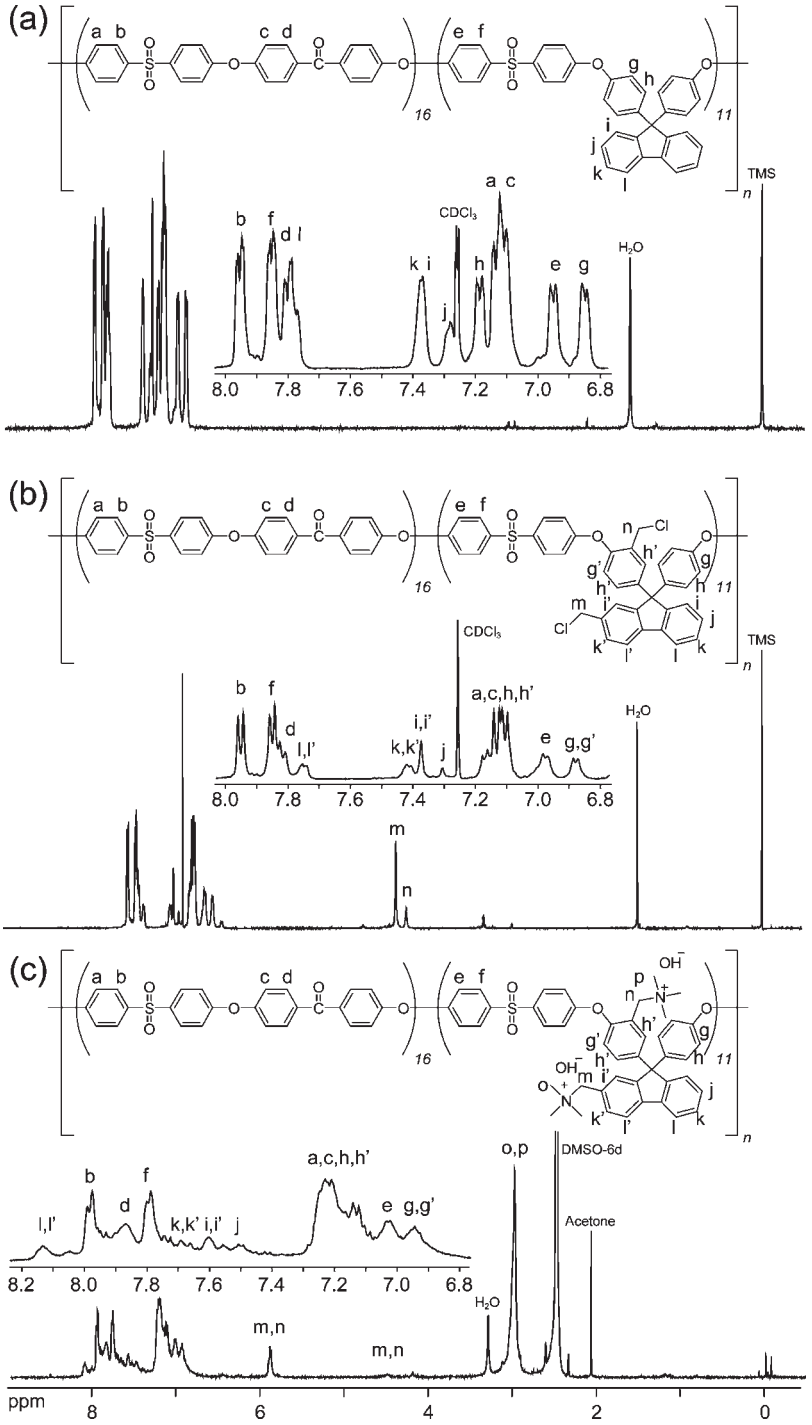

Figure 1. ^{1}H NMR spectra of (a) PE-*X*16*Y*11, (b) CMPE-*X*16*Y*11, and (c) QPE-*X*16*Y*11 (IEC = 1.52 meq/g).

dx.doi.org/10.1021/ja204166e |*J. Am. Chem. Soc.* 2011, 133, 10646–10654

Scheme 2. Chloromethylation and Quaternization Reactions of PEs

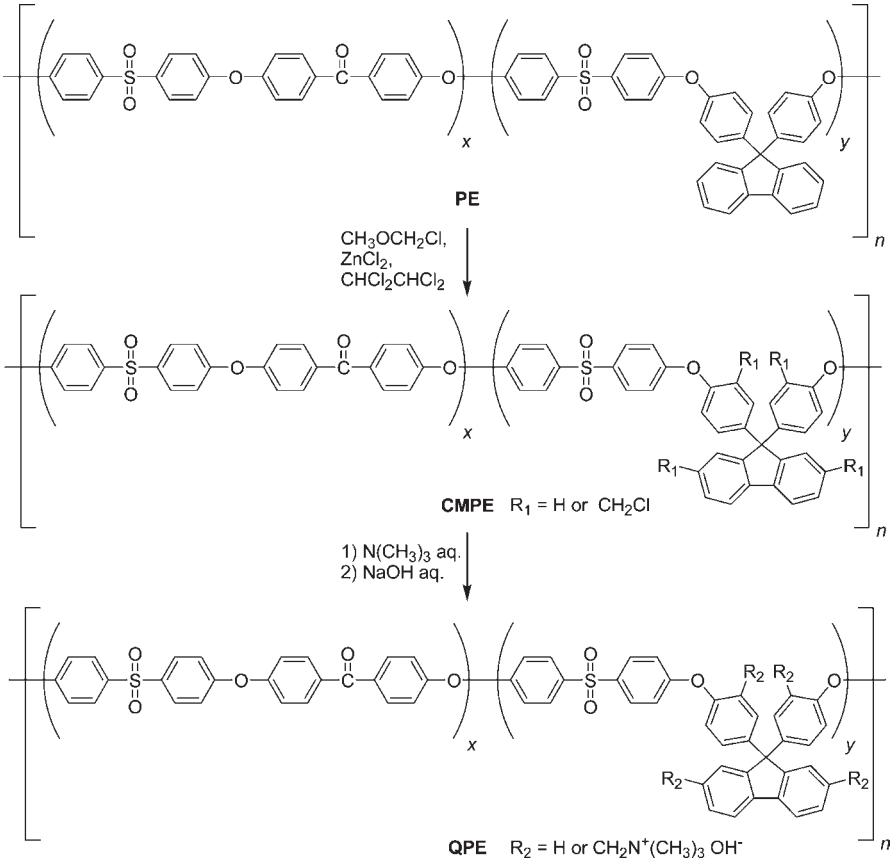

The oligomer lengths were determined from the integral ratio of the protons at the terminal phenyl groups to those in the repeat units in the ^{1}H NMR spectra. The oligomer lengths obtained were shorter than the expected ones from the monomer feed ratios when *X* and *Y* were large (>16). Since the oligomerization reaction was terminated in a rather short time (4−5 h) in order to avoid unfavorable side reactions, the resulting end-capped oligomers were of lower molecular weight.

Block copolymerization was carried out with an equimolar amount of hydrophobic and fluorene-containing oligomers in the presence of potassium carbonate and calcium carbonate in dry DMAc solution. A combination of oligomers with different block lengths provided a series of multiblock PEs (PE-*X*8*Y*8, -*X*16*Y*8, -*X*22*Y*11, and -*X*22*Y*23). The PEs obtained were soluble in some organic solvents such as chloroform, dichloromethane, 1,1,2,2-tetrachloroethane, *N*,*N*-dimethylformamide (DMF), DMAc, and dimethylsulfoxide (DMSO). The molecular weights of the PEs were measured by GPC, in which the elution curves were unimodal. As summarized in Table 1, the PEs were of high molecular weight (M_w > 93 kg/mol, M_n > 54 kg/mol), providing transparent, ductile membranes by solution casting. The molecular weights of the PEs were several times higher than those of the starting oligomers, indicating successful formation of multiblock copolymers. The ^{1}H NMR spectra of the multiblock copolymers were well-assigned to the assumed chemical structure (Figure 1a as an example for PE-*X*16*Y*11) by referring to the spectra of the starting oligomers (Figure S1, SI). The copolymer composition was in good agreement with the oligomer feed ratio, further supporting the multiblock structure.

Synthesis and Characterization of Chloromethylated Multiblock Copoly(arylene ether)s (CMPEs). The Friedel−Crafts chloromethylation reaction of the PEs was carried out with chloromethyl methyl ether (CMME) and a Lewis acid catalyst in 1,1,2,2-tetrachloroethane solution (Scheme 2). Since the chloromethylation reaction is often accompanied by a slight but undesirable cross-linking reaction of the resulting chloromethyl groups and causes gelation of the mixture, the reaction conditions had to be carefully controlled. In our previous study, we searched the reaction conditions in detail with homopolymers and random copoly(arylene ether)s in terms of temperature and amount of CMME.[25] The optimized conditions were at 35 °C and 40 equiv of CMME to achieve a high degree of chloromethylation (number of substituted chloromethyl groups per repeat unit in the fluorene-containing block) without gelation. The degree of chloromethylation was controllable by changing the reaction time. The optimized reaction conditions were applied to the multiblock PEs. In addition, because of the better solvent solubilities of multiblock PEs than those of homopolymers and random copolymers, somewhat wider reaction conditions were available, with temperatures up to 45 °C and equivalents of CMME up to 80.

The chemical structure and the degree of chloromethylation of the chloromethylated PEs (CMPEs) were analyzed by ^{1}H NMR spectra. In the ^{1}H NMR spectrum of CMPE-*X*16*Y*11 (Figure 1b), a peak assignable to the methylene protons of the chloromethyl groups was observed at 4.58 ppm, which was absent in the ^{1}H NMR spectrum of the precursor PE-*X*16*Y*11 (Figure 1a). The substitution of the chloromethyl groups on PEs

dx.doi.org/10.1021/ja204166e |*J. Am. Chem. Soc.* 2011, 133, 10646–10654

altered several peaks between 7.9 and 7.2 ppm, which were derived from the fluorenyl biphenylene protons. The integral value of the peaks at 7.30 ppm, assignable to the protons at the 2- and 7-positions of the fluorene groups (denoted as j in Figure 1a and b), was smaller for CMPE than that for PE. The integral value of the newly appeared peak at 4.58 ppm was coincident with that of the decreasing peaks at 7.30 ppm. An adjacent peak at 4.45 ppm was assigned to the methylene protons of the chloromethyl groups on the polymer main chain (denoted as g in Figure 1b). The ^{1}H NMR spectrum suggested that the chloromethyl groups were preferentially substituted at specific positions, i.e., the 2- and 7-carbons of the fluorene groups (denoted as j in Figure 1a) and the phenylene carbons ortho to the ether bonds in the fluorenylidene biphenylene unit (denoted as g in Figure 1a). There was no evidence for the chloromethylation of the hydrophobic blocks. The results were reasonable, taking into account the fact that all phenylene rings were bonded with electron-withdrawing groups in the hydrophobic blocks. Similar results were obtained for the electrophilic sulfonation reaction of the same multiblock copoly(arylene ether)s.[27,28] The degree of chloromethylation in CMPE was estimated from the integral ratio of the methylene protons of the chloromethyl groups (4.45−4.58 ppm) to the protons of the 4-positional protons at the fluororene groups (denoted as l in Figure 1b) and the phenylene protons meta to the ether bonds in the biphenyl sulfone (denoted as b and f in Figure 1b) and ketone (denoted as d in Figure 1b) at 7.7−8.0 ppm. These aromatic protons were chosen due to their inactivity to the electrophilic chloromethylation reaction.

The degree of chloromethylation was controllable by changing the reaction conditions. As shown in Figure 2a, the degree of chloromethylation of CMPE-*X*16*Y*11 increased with the reaction time, and the highest value (2.78) was achieved by an 144-h reaction at 45 °C with 80 equiv of CMME. The degree of chloromethylation was plotted as a function of time for four different conditions. Both the reaction temperature and the equivalents of CMME were influential parameters on the degree of chloromethylation. It should be noted that a large excess (80 equiv) of volatile CMME (bp = 59 °C) was needed for a high degree of chloromethylation at 45 °C. In Figure 2b is plotted the degree of chloromethylation in the CMPE-*X*16*Y*11 separately for the main chains and the fluorene groups, in addition to the total values. The fluorene groups were more reactive than the main chains due to the lack of electron-withdrawing ketone and sulfone groups. The fluorene groups were selectively and quantitatively chloromethylated at the 2 and 7 positions, while the number of chloromethyl groups in the main chains did not exceed one even after the 144-h reaction. Longer reaction times and/or severer reaction conditions failed to achieve a higher chloromethylation degree in the main chains but resulted in gelation. Nevertheless, the total degree of chloromethylation was much higher than that of our random copolymers.[24,25] The results of the chloromethylation reactions of the four multiblock copolymers are summarized in Table 2.

Membrane Formation and Quaternization of CMPEs. The CMPEs were cast from 1,1,2,2-tetrachloroethane solutions to provide membranes. The membranes obtained were colorless, transparent, tough, and ductile. The thickness was controlled to be 50 μm. The CMPE membranes were converted to quaternized ammonio forms by treating with trimethylamine aqueous solution (Scheme 2). The subsequent immersion of the membranes in sodium hydroxide aqueous solution provided quaternized multiblock

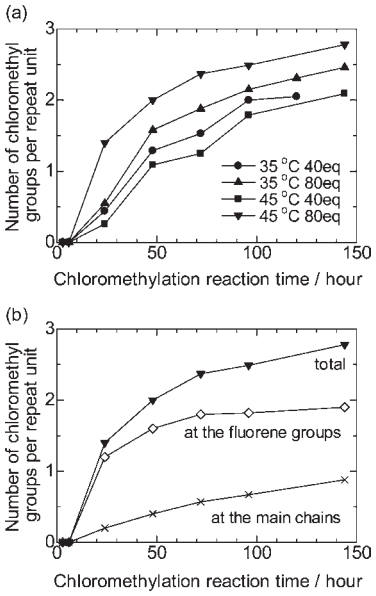

Figure 2. Time dependence of the degree of chloromethylation in CMPE-*X*16*Y*11 (a) under various conditions and (b) at 45 °C and 80 eq. of CMME.

copoly(arylene ether) (QPE) membranes with hydroxide counteranions. The QPE membranes were pale yellow and transparent and showed lower solubilities in organic solvents than those of the parent CMPEs. The QPE membranes in the OH^- form were soluble in DMSO, and those in the Cl^- form were soluble in DMF and DMAc when their IEC was lower than 1.5 meq/g. They were not soluble in less polar solvents such as halogenated hydrocarbons. The multiblock QPEs showed better solubilities than the rQPEs. The latter in the Cl^- form were not soluble in any solvents examined.[25]

The chemical structures of the QPEs were analyzed by ^{1}H NMR spectra. In Figure 1c is shown the ^{1}H NMR spectrum of QPE-*X*16*Y*11 (IEC = 1.52 meq/g). A strong peak at 2.96 ppm was assigned to the methyl groups on the quaternized ammonio groups (denoted as o and p in Figure 1c). The sharp peaks of methylene protons at 4.45 and 4.58 ppm in CMPE-*X*16*Y*11 (Figure 1b) shifted to lower magnetic field at 5.90 ppm as a single peak in QPE-*X*16*Y*11 (Figure 1c). We found that another peak appeared occasionally at 4.92 ppm even for the same samples. These two peaks were both assigned to the ammonio-substituted methylene protons, because the sum of the integral ratios of the two peaks was constant. It is reasonably assumed that transformation of hydroxide ions to carbonate and/or bicarbonate ions by contact with a trace amount of carbon dioxide in the air caused the shift of the methylene protons to higher magnetic field.[33] The integral ratio of the methyl proton peak at 2.96 ppm (or methylene proton peaks at 5.90 and 4.92 ppm) to aromatic proton peaks at 6.8−8.2 ppm indicated that the quaternization reaction was quantitative. This was further supported by the absence of chloromethylene proton peaks at 4.45 and 4.58 ppm. The ion-exchange capacity (IEC) of the QPE-*X*16*Y*11 membrane was calculated to be 1.54 meq/g from the integral ratio, which was in good agreement with the calculated value (1.52 meq/g) from the copolymer composition and the degree of chloromethylation, assuming the complete quaternization of the chloromethyl groups. The IEC values calculated from the NMR spectra and the copolymer compositions of the other QPE membranes are summarized in Table 2. The experimental IEC values (from NMR)

Table 2. Degree of Chloromethylation in CMPEs, and IEC, Water Uptake, λ, and Hydroxide Ion Conductivity of QPE Membranes

membrane	degree of chloromethylation[a]	IEC[b] (meq/g)	IEC[c] (meq/g)	water uptake (%)	λ[d]	hydroxide ion conductivity at 60 °C (mS/cm) in water
QPE-*X*8*Y*8	0.43	0.44	0.39	26	32.8	2.4
	0.92	0.89	0.82	58	36.2	14
	1.35	1.26	1.15	70	30.8	42
	1.57	1.44	1.44	95	36.6	56
	2.17	1.83	1.71	92	27.9	90
QPE-*X*16*Y*11	1.13	0.82	0.79	19	12.9	8.8
	1.73	1.29	1.13	29	12.5	47
	1.78	1.32	1.38	29	12.2	52
	2.09	1.52	1.54	50	18.3	93
	2.78	1.93	2.05	112	32.2	126
QPE-*X*22*Y*11	0.92	0.89	0.86	18	11.2	25
	2.19	1.37	1.32	38	15.4	83
	2.81	1.70	1.72	58	18.9	121
QPE-*X*22*Y*23	1.84	1.62	1.65	62	21.2	126
rQPE	0.39	0.68	–	21	17.1	0.3
	0.75	1.23	–	61	27.5	9.0
	1.24	1.88	–	95	28.0	35

[a] Number of substituted chloromethyl groups per repeat unit in the fluorene-containing block. [b] Calculated from the copolymer composition and the degree of chloromethylation. [c] Estimated from the ^{1}H NMR spectra. [d] Number of absorbed water molecules per ammonium group: λ = [water uptake (g/g)/18.02 (g/mol)] × [1000/IEC (meq/g)]

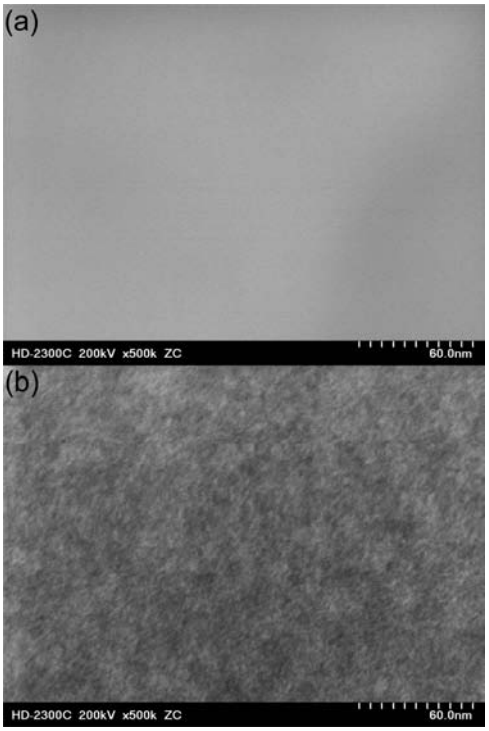

Figure 3. STEM images of (a) rQPE (IEC = 1.88 meq/g) and (b) QPE-*X*16*Y*11 (IEC = 1.52 meq/g) stained with tungstate ions.

were comparable to the calculated values within acceptable errors in all QPE membranes.

Morphologies of QPE Membranes. In order to analyze the hydrophilic/hydrophobic phase separation, STEM images were taken for the multiblock QPE membranes and compared with those of the rQPE membranes. In Figure 3 are shown STEM images of the QPE-*X*16*Y*11 (IEC = 1.52 meq/g) and rQPE (IEC = 1.88 meq/g) membranes stained with tungstate ions as typical examples. The rQPE membrane showed a uniformly gray image throughout the field of view, suggesting no distinct phase separation. In contrast, the QPE-*X*16*Y*11 membrane showed a phase-separated morphology. The dark ionic (ammonium-containing) domains, with widths of ~5 nm, were distributed in the membrane. Similar images were obtained in the other QPE membranes. Figure S2 in SI shows a TEM image of QPE-*X*22*Y*11 (IEC = 0.89 meq/g) membrane, in which spherical ionic domains with 4−5 nm in diameter were observed in clear contrast. It is considered that the developed hydrophilic/hydrophobic phase separation is caused by the sequential block structure despite its lower IEC value or ionic concentration than that of rQPE. A similar effect was also observed in our PEMs containing sulfonated fluorene groups.[27,28] The size of ionic domains observed in the QPE membranes was smaller compared with the length of hydrophilic blocks. The polymer main chains could fold with close packing due to strong intermolecular interactions of aromatic groups. Since the QPE membranes were obtained by the quaternization of precast CMPE membranes, the phase-separated morphology would basically stem from the structural differences between the blocks of phenylene sulfone and chloromethylated fluorene groups and those of the phenylene sulfone-*co*-ketone units. It should be noted that the quaternization and the ion-exchange procedures could affect the morphology to a greater or lesser degree, since the hydrophilic QPE membranes swell in water, as discussed below, and gain flexibility.

Water Uptake and Hydroxide Ion Conductivity of QPE Membranes. Water uptake (30 °C) and hydroxide ion conductivities (40 °C) of the QPE membranes were measured in water and plotted as a function of IEC in Figure 4. Water uptake of the QPE membranes increased with increasing IEC. A comparison of multiblock and random QPE membranes revealed that the multiblock QPE membranes, except for the QPE-*X*8*Y*8 membranes,

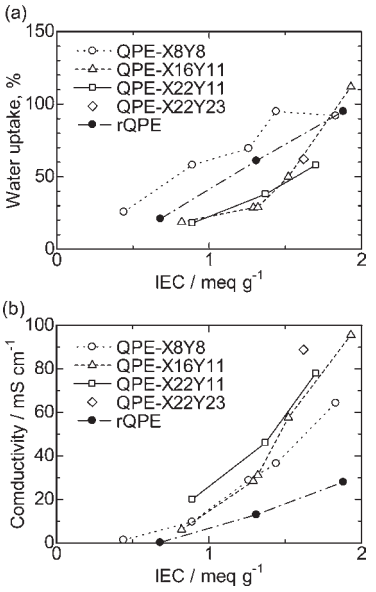

Figure 4. (a) Water uptake at 30 °C and (b) hydroxide ion conductivity at 40 °C of QPE membranes as a function of ion-exchange capacity (IEC).

absorbed less water. For a better comparison among the different IEC membranes, the number of absorbed water molecules per ammonium group (designated as λ) was calculated (Table 2). The approximate trend was that water uptake increased with IEC and decreased with block length. Since the water uptake and λ value of rQPE (95% and 28.0, respectively, for IEC = 1.88 meq/g) were comparable to those of the reported AEMs composed of aromatic polymers bearing quaternized ammonio groups (e.g., ~95% and 28.9 for IEC = 1.89 meq/g[16] and ~115% and 29.0 for IEC = 2.2 meq/g[17]), lower water uptake and λ values of the multiblock QPE membranes are considered to be related to the developed hydrophilic/hydrophobic phase-separated morphology. The developed hydrophobic domains composed of longer sequences could contribute to suppression of excessive water uptake and swelling.

Similar to the water uptake, the hydroxide ion conductivity of the multiblock QPE membranes increased with increasing IEC. The three QPE membranes, *X*16*Y*11, *X*22*Y*11, and *X*22*Y*23 showed similar conductivity dependence on the IEC values. The QPE-*X*16*Y*11 membrane with IEC = 1.93 meq/g showed the highest conductivity (96 mS/cm). The temperature dependence of the hydroxide ion conductivities of the QPE-*X*16*Y*11 and rQPE membranes in water is compared in Figure 5. Similar to the results in Figure 4, the conductivities followed the order of the IEC values for the same series of QPE and rQPE. The QPE-*X*16*Y*11 membrane (IEC = 1.93 meq/g) showed the highest conductivity (144 mS/cm) at 80 °C, which was ~3.2 times higher than that of the rQPE membrane with IEC = 1.88 meq/g under the same conditions.[25] To the best of our knowledge, the QPE-*X*16*Y*11 (IEC = 1.93 meq/g) membrane shows the highest hydroxide conductivity reported thus far for anion conductive membranes.[10−23] The important point is that the multiblock QPE membranes showed a lower water uptake but considerably higher conductivity than those of the random QPE membranes. These results suggest that our concept to apply the multiblock structure with highly ionized hydrophilic blocks is effective for the AEMs for improving the ionic conductivity, as already

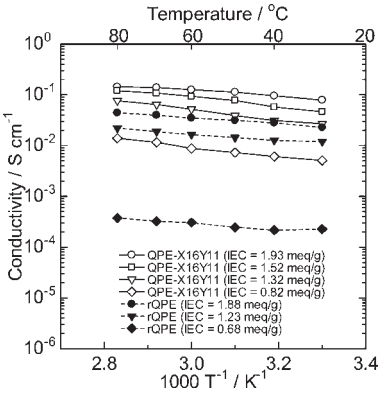

Figure 5. Temperature dependence of hydroxide ion conductivities of QPE-*X*16*Y*11 and rQPE membranes.

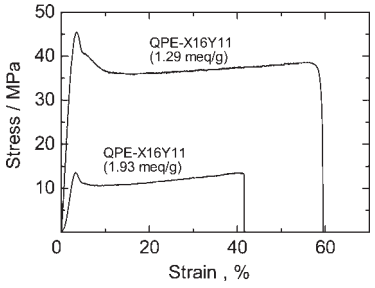

Figure 6. Stress versus strain curves of *X*16*Y*11 membranes (IEC = 1.29 and 1.93 meq/g) at 80 °C and 60% RH.

demonstrated for PEMs. Due to the well-developed phase-separated morphology, multiblock QPE membranes can utilize water molecules more efficiently for hydroxide ion transport.

The conductivities of the QPE membranes showed an approximate Arrhenius-type temperature dependence. The apparent activation energy estimated from the slopes was ~10 kJ/mol and was similar among the tested membranes. The apparent activation energy of the QPEs was comparable or somewhat lower than those of reported AEMs (9.92−23.03 kJ/mol),[14−21] implying that these membranes share a similar hydroxide ion conduction mechanism involving the hydrated ions.

Stability of QPE membranes. The mechanical stabilities of the QPE-*X*16*Y*11 membranes (IEC = 1.29 and 1.93 meq/g) were measured at 80 °C and 60% RH by use of a universal testing instrument (Figure 6). The conditions were chosen so as to simulate the below mentioned fuel cell operating conditions, however, the humidity was lower to minimize experimental errors. A low IEC membrane showed a higher mechanical strength (45 MPa maximum strength, 59% strain at break, and 1.2 GPa initial Young's modulus) than that of a high IEC membrane (13 MPa maximum strength, 41% strain at break, and 0.4 GPa initial Young's modulus). These results are reasonable taking into account the higher water absorbability (higher swellability) of the higher IEC membrane (Table 2). The mechanical properties of the QPE membranes were similar to those of the rQPE membranes,[25] and appeared to be dependent on the IEC rather than the sequential main chain structure. In other words, the multiblock QPE membranes were not as mechanically strong as expected from their rather low water absorbability. Similar behavior has been observed in our multiblock PEMs.[26]

A serious issue for the AEMs is their chemical instability compared to that of the PEMs. Under heated or hydrothermal conditions, possible degradation mechanisms for AEMs have been discussed in the literature.[32,33] There are four major degradation modes: (1) elimination of a tertiary amine to form benzyl alcohol, (2) a Stevens rearrangement to form 2-(*N*,*N*-dimethylamino)ethylbenzene, (3) rearrangement of the methyl group to form 1-(*N*,*N*-dimethylamino)ethylbenzene, and (4) a Sommelet−Hauser rearrangement to form 2-(*N*,*N*-dimethylamino)methyltoluene (Figure S3 in SI). To evaluate the stability and degradation mechanism of the multiblock QPE membranes, QPE-*X*16*Y*11 (IEC = 1.65 or 1.75 meq/g) membrane was treated in hot water or hot air at 80 °C for 500 h, respectively. The membranes maintained its toughness, flexibility, and appearance after both stability tests. The chemical structures before and after the tests were analyzed by use of ^{1}H NMR spectra (Figures S4 and S5 in SI). After the hydrothermal test in hot water, the peaks for the methyl and methylene protons (denoted as o,p and m,n in Figure S4, SI) became smaller, while the aromatic proton peaks between 8.2−6.8 ppm showed minor changes (Figure S4b, SI) when compared with those of the pristine sample (Figure S4a, SI). The IEC value estimated from the integral ratio of methyl groups after the hydrothermal test was 1.44 meq/g, which was slightly smaller than that of the initial QPE (IEC = 1.65 meq/g). In contrast, ^{1}H NMR spectrum of QPE-*X*16*Y*11 after the thermal test in hot air showed larger decrease in methyl and methylene protons (Figure S5b). The IEC value after the test was estimated to be 1.09 meq/g, which was ∼60% of the initial value. Since no other peaks assignable to methyl, methylene, or methyne protons,[33] which are assumed to appear in the degradation mechanisms 2−4 in Figure S3, SI, were observed in Figures S4b and S5b, SI, major degradation mode of QPE membranes in the thermal and hydrothermal tests is the most likely to involve the mechanism 1), that is the elimination of a tertiary amine to form benzyl alcohol (Figure S3, SI). Benzyl alcohol could be further decomposed via dehydration as implied by TG/DTA-Ms analyses of our rQPE.[25] These results revealed that dry and hot conditions negatively affected to some extent the QPE membranes to reduce their IEC values by the elimination of the tertiary amine groups, while the hydrothermal conditions were less harmful to the QPE membranes.

The long-term durability of the QPE membranes in hot water was further investigated in terms of the hydroxide ion conductivity. The hydroxide ion conductivities of the QPE-*X*8*Y*8 (IEC = 1.26 meq/g) membrane are plotted as a function of time in Figure 7. After an initial period of transient behavior for several tens of hours, the conductivity showed a constant but slow decline starting from 36 mS/cm. The decay rate was as low as 1.9 μS/h on average. The membrane retained its toughness and flexibility after 5000 h. The chemical structures before and after the tests were also analyzed by ^{1}H NMR spectra (Figure S6, SI). Though the peaks for the methyl and methylene protons became smaller after 5000 h in hot water, the IEC value estimated from the integral ratio was 1.03 meq/g, which was 82% of the initial IEC. This IEC drop was consistent with the conductivity decline. Since the conductivity became constant after several tens hours, the high durability of the QPE membrane appears promising for application in alkaline fuel cells.

Fuel Cell Performance. We have been working on noble metal-free anion-exchange membrane fuel cells.[34,35] They can be operated with hydrazine (hydrate) as a fuel instead of hydrogen gas for typical PEM fuel cells.[36] Abundant transition metal-based

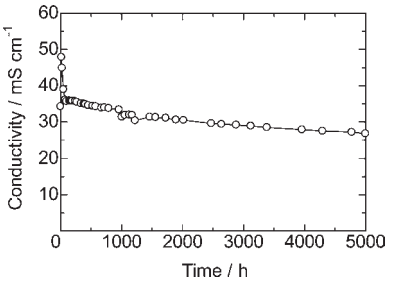

Figure 7. Time course of hydroxide ion conductivity of the QPE-*X*8*Y*8 (IEC = 1.26 meq/g) membrane in pure water at 80 °C.

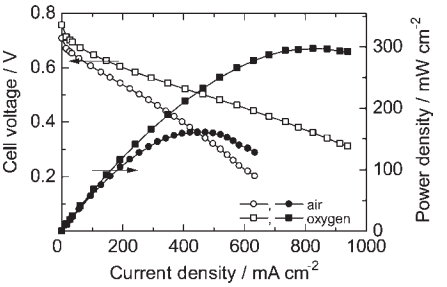

Figure 8. Direct hydrazine fuel cell performance (cell voltage and power density versus current density) of the QPE-*X*16*Y*11 (IEC = 1.93 meq/g) membrane with air or oxygen at 80 °C.

catalysts are suitable for both electrodes. In a typical case, Ni powder and Co with poly(pyrrole) dispersed on carbon are used for the anode and the cathode, respectively. These advantages are attractive for automotive applications. The QPE-*X*16*Y*11 (IEC = 1.93 meq/g) membrane was used in a hydrazine fuel cell, in which KOH was added in the fuel to prevent the formation of hydrazinium ions ($N_2H_5^+$) at the anode and to facilitate the oxygen reduction reaction at the cathode.[35] Hydroxide ion conductivity of the membrane could also be improved to some extent. The fuel cell performance is shown in Figure 8. The open circuit voltage (OCV) was 0.71 V (with air) and 0.76 V (with oxygen), which is lower than that of typical hydrogen-supplied fuel cells (∼1.0 V) because of the hydrazine hydrate crossing over to the cathode through the membrane (the permeability of hydrazine was measured ex situ to be 2.3 g mm/m^2 h at 30 °C). Reasonably high fuel cell performance was obtained with the maximum power density of 161 mW/cm^2 at a current density of 446 mA/cm^2 with air and 297 mW/cm^2 at 826 mA/cm^2 with oxygen. The optimization of the catalysts and the MEA fabrication procedure is in our future agenda for further improving the performance.

CONCLUSIONS

A series of anion-conductive multiblock poly(arylene ether)s containing ammonium-functionalized fluorene groups was designed and synthesized. By carefully optimizing the reaction conditions, precursor multiblock copolymers were chloromethylated selectively at specific positions on the fluorene-containing units. The chloromethylation of the fluorene groups was nearly complete because of their high electron density, while that on the main chains was up to half, which accounted for 2.78 chloromethyl groups per repeat unit. Quaternization and the subsequent ion-exchange reactions were quantitative, resulting in QPE

membranes with IEC values up to 1.93 meq/g. The QPE membrane showed distinct hydrophilic/hydrophobic phase separation, as confirmed by STEM images. The QPE-*X*16*Y*11 membrane with the highest IEC showed very high hydroxide ion conductivity (144 mS/cm) at 80 °C. The QPE membranes were mechanically and chemically stable, similar to the random QPE membranes composed of the same repeat unit. Thus, it was confirmed that the concept to utilize a multiblock copolymer structure with highly ionized hydrophilic blocks is effective for improving the ionic conductivity of AEMs without sacrificing other desirable properties such as mechanical stability. The QPE membrane showed reasonable performance in a noble metal-free fuel cell with hydrazine hydrate. Selection of the electrocatalysts and electrode preparation can be optimized to further improve the fuel cell performance.

■ ASSOCIATED CONTENT

Supporting Information. Experimental section, complete ref 3, TEM image of QPE-*X*22*Y*11 (IEC = 0.89 meq/g), ^{1}H NMR spectra of oligomers and polymers, GPC data of oligomers, and possible degradation mechanisms of AEMs. This material is available free of charge via the Internet at http://pubs.acs.org.

■ AUTHOR INFORMATION

Corresponding Author

miyatake@yamanashi.ac.jp (K.M.); m-watanabe@yamanashi.ac.jp (M.W.)

Present Address

[||]Department of Applied Chemistry, Tokyo Metropolitan University, Hachioji, Tokyo 192-0397, Japan.

■ ACKNOWLEDGMENT

This work was partly supported by the Ministry of Education, Culture, Sports, Science and Technology Japan through a Grant-in-Aid for Scientific Research (22760536, 23350089, and 23656427).

■ REFERENCES

(1) Vielstich, W. *Handbook of Fuel Cells*; Wiley: Chichester, England, 2009.
(2) Carrette, L.; Friedrich, K. A.; Stimming, U. *Fuel Cells* **2001**, *1*, 5–39.
(3) Borup, R.; et al. *Chem. Rev.* **2007**, *107*, 3904–3951.
(4) Vorcoe, J. R.; Slade, R. C. T. *Fuel Cells* **2005**, *2*, 187–200.
(5) Xu, T. *J. Membr. Sci.* **2005**, *263*, 1–29.
(6) Hickner, M. A. *Mater. Today* **2010**, *13*, 34–41.
(7) Olson, T. S.; Pylypenko, S.; Atanassov, P.; Asazawa, K.; Yamada, H.; Tanaka, H. *J. Phys. Chem. C* **2010**, *114*, 5049–5059.
(8) Sanabria-Chinchilla, J.; Asazawa, K.; Sakamoto, T.; Yamada, K.; Tanaka, T.; Strasser, P. *J. Am. Chem. Soc.* **2011**, *133*, 5425–5431.
(9) Robertson, N. J.; Kostalik, H. A., IV; Clark, T. J.; Mutolo, P. F.; Abruña, H. D.; Coates, G. W. *J. Am. Chem. Soc.* **2010**, *132*, 3400–3404.
(10) Varcoe, J. R.; Slade, R. C. T.; Yee, E. L. H.; Poynton, S. D.; Driscoll, D. J.; Apperley, D. C. *Chem. Mater.* **2007**, *19*, 2686–2693.
(11) Zeng, Q. H.; Liu, Q. L.; Broadwell, I.; Zhu, A. M.; Xiong, Y.; Tu, X. P. *J. Membr. Sci.* **2010**, *349*, 237–243.
(12) Luo, Y.; Guo, J.; Wang, C.; Chu., D. *J. Power Sources* **2010**, *195*, 3765–3771.
(13) Wu, L.; Zhou, G.; Liu, X.; Zhang, Z. H.; Li, C.; Xu, T. *J. Membr. Sci.* **2011**, *371*, 155–162.
(14) Hibbs, M. R.; Fujimoto, C. H.; Cornelius, C. J. *Macromolecules* **2009**, *42*, 8316–8321.
(15) Wang, G.; Weng, Y.; Chu, D.; Xie, D.; Chen, R. *J. Membr. Sci.* **2009**, *326*, 4–8.
(16) Hibbs, M. R.; Hickner, M. A.; Alam, T. M.; McIntyre, S. K.; Fujimoto, C. Y.; Cornelius, C. J. *Chem. Mater.* **2008**, *20*, 2566–2573.
(17) Zhou, J.; Unlu, M.; Vega, J. A.; Kohl, P. A. *J. Power Sources* **2009**, *190*, 285–292.
(18) Wang, J.; Li, S.; Zhang, S. *Macromolecules* **2010**, *43*, 3890–3896.
(19) Yan, J.; Hickner, M. A. *Macromolecules* **2010**, *43*, 2349–2356.
(20) Gu, S.; Cai., R.; Yan, Y. *Chem. Commun.* **2011**, 2856–2858.
(21) Zhao, Z.; Wang, J.; Li, S.; Zhang, S. *J. Power Sources* **2011**, *196*, 4445–4450.
(22) Xiong, Y.; Liu, Q. L.; Zhu, A. M.; Huang, S. M.; Qing, Zeng, H. *J. Power Sources* **2009**, *186*, 328–333.
(23) Wu, Y.; Wu, C.; Varcoe, J. R.; Poynton, S. D.; Wu, T.; Fu, Y. *J. Power Sources* **2010**, *195*, 3069–3076.
(24) Tanaka, M.; Koike, M.; Miyatake, K.; Watanabe, M. *Macromolecules* **2010**, *43*, 2657–2659.
(25) Tanaka, M.; Koike, M.; Miyatake, K.; Watanabe, M. *Polym. Chem.* **2011**, *2*, 99–106.
(26) Bae, B.; Miyatake, K.; Watanabe, M. *ACS Appl. Mater. Interfaces* **2009**, *1*, 1279–1286.
(27) Bae, B.; Yoda, T.; Miyatake, K.; Uchida, H.; Watanabe, M. *Angew. Chem., Int. Ed.* **2010**, *49*, 317–320.
(28) Bae, B.; Miyatake, K.; Watanabe, M. *Macromolecules* **2010**, *43*, 2684–2691.
(29) Lee, H. S.; Roy, A.; Lane, O.; Lee, M.; McGrath, J. E. *J. Polym. Sci., Part A: Polym. Chem.* **2010**, *48*, 214–222.
(30) Peckham, T. J.; Holdcroft., S. *Adv. Mater.* **2010**, *22*, 4667–4690.
(31) Elabd, Y. A.; Hickner, M. A. *Macromolecules* **2011**, *44*, 1–11.
(32) Chempath, S.; Einsla, B. R.; Pratt, L. R.; Macomber, C. S.; Boncella, J. M.; Rau, J. A.; Pivovar, B. S. *J. Phys. Chem. C* **2008**, *112*, 3179–3182.
(33) Chempath, S.; Boncella, J. M.; Pratt, L. R.; Henson, N.; Pivovar, B. S. *J. Phys. Chem. C* **2010**, *114*, 11977–11983.
(34) Asazawa, K.; Yamada, K.; Tanaka, H.; Oka, A.; Taniguchi, M.; Kobayashi, T. *Angew. Chem., Int. Ed.* **2007**, *46*, 8024–8027.
(35) Asazawa, K.; Sakamoto, T.; Yamaguchi, S.; Yamada, K.; Fujikawa, H.; Tanaka, H.; Oguro, K. *J. Electrochem. Soc.* **2009**, *156*, B509–B512.
(36) Serov, A.; Kwak, C. *Appl. Catal., B* **2010**, *98*, 1–9.